

Numerical Simulation of Autodoping Profiles  
in Silicon Epitaxy

M. Wong, R. Reif

Department of Electrical Engineering and Computer Science  
Massachusetts Institute of Technology  
Cambridge, MA 02139

G. R. Srinivasan

I.B.M. East Fishkill Facility  
Hopewell Junction, NY 12533

ABSTRACT

The phenomenon of autodoping refers to the unintentional doping of the epitaxial layer. It is most prominent when intrinsic (or lightly doped) films are deposited on heavily doped substrates.

A model of arsenic autodoping in silicon epitaxy is proposed. The model is characterized by four parameters. Three of them are related to the dopant incorporation process. The fourth one has the nature of an initial condition to the model equation.

The model has been numerically implemented. With properly specified parameters, it gives good simulations of autodoping profiles obtained from a variety of sources.

1: INTRODUCTION

In the continual drive to scaling devices, it becomes necessary to fabricate very thin epitaxial layers. Since the growth times associated with thin film depositions can be comparable to the transient time associated with the doping of the films, complicated doping profiles may appear in thin films. Accurate predictions of these doping profiles requires thorough understanding of the transient response of CVD systems.

Transient profiles also appear in places where they

normally are not desired. One prominent example is the unintentional doping of an intrinsic (or lightly doped) epitaxial layer deposited on a heavily doped substrate. "Autodoping" is the name given to this kind of transient effects.

Traditionally, autodoping has been described by a sequence of processes that begin with the evaporation of impurities into the gas phase. These evaporated impurities are either re-incorporated into the growing epitaxial layer, or transported by the carrier gas before being re-incorporated in other parts of the growing epitaxial layer. These re-incorporated atoms are responsible for the phenomenon of autodoping.

In more recent investigations of autodoping [3], [8], the role of surface adsorbed impurities has been emphasized. This approach not only provides a physical understanding of autodoping, but also enables quantitative predictions of autodoping profiles.

It will be shown that the only parameter generic to the modeling of autodoping is the density of impurity atoms adsorbed on the surface of the substrate immediately before actual deposition.

## 2: THE DOPANT INCORPORATION MODEL

### 2.1: physical description

The dopant incorporation process can be partitioned into the following steps [3]:

- a) Transport of dopant carriers to the surface.
- b) Adsorption of dopant carriers on the substrate surface.
- c) Chemical decomposition of dopant carriers.
- d) Surface diffusion of dopant atoms to incorporation sites.
- e) Covering of dopant atoms by silicon atoms.

In the subsequent computer implementation of the model [4], some of the physics involved in the covering step was lost in the mathematical representation of the physical model. Specifically, instead of relating the amount of adsorbed impurities to the doping concentration in the epitaxial layer to be deposited on the surface (as is suggested by a "covering" mechanism), the derived equation in [4] relates it to the doping concentration just below the surface (through the equilibrium constant  $K_A$ ).

The following modifications to the covering step (e) are made:

- e1) A layer of silicon atoms is deposited.
- e2) A fraction of the impurities adsorbed on the original surface is trapped in the layer, thus incorporated.
- e3) The rest relaxes onto the growing surface.

The purpose of these modifications is to enable the reformulation of the model equation in terms of a parameter that emphasizes the role of impurities adsorbed on the surface, i.e. the density of impurities adsorbed on the surface at any given instant. This facilitates the derivation of a better mathematical representation of the "covering" process.

## 2.2: mathematical description

Consider a growing epitaxial layer at some instant  $t = t_0$  (Figure 1). The density of dopant atoms adsorbed on the surface is given by  $N_A$  (per unit area). Let the growth rate be denoted by  $g$ , then at an instant  $dt$  later, a layer of silicon of thickness  $dx (= gdt)$  is deposited. This situation is depicted in Figure 2.

The impurity atoms adsorbed on the "old" surface:

- a) either are trapped in the layer, thus becoming incorporated,
- b) or relax onto the "new" surface, thus contributing in part to the new surface adsorption density.

We introduce the trapping factor  $f$ , which can be interpreted as the probability per unit thickness (Appendix A) that an atom adsorbed on the surface of a growing film is trapped. Therefore, the probability that an impurity atom be trapped in an epitaxial layer of thickness  $dx$  is given by  $f dx$ . The equation:

$$(1): dN_A^t = N_A f dx$$

relates the amount  $dN_A^t$  trapped in the layer  $dx$  to the amount  $N_A$  adsorbed on the "old" surface.

If it is assumed that the exchange of impurities between the surface and the underlying bulk material is negligible during the time interval  $dt$ , then  $dN_A^t$  is also given by  $C_s dx$ , where  $C_s$  is the concentration of impurities in the layer  $dx$ . The following relationship is then established:

$$(2): C_s = f N_A$$

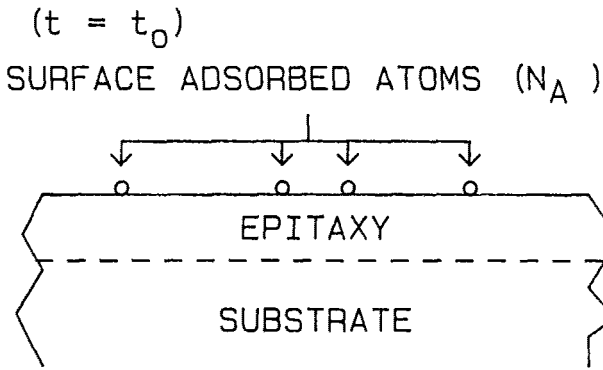
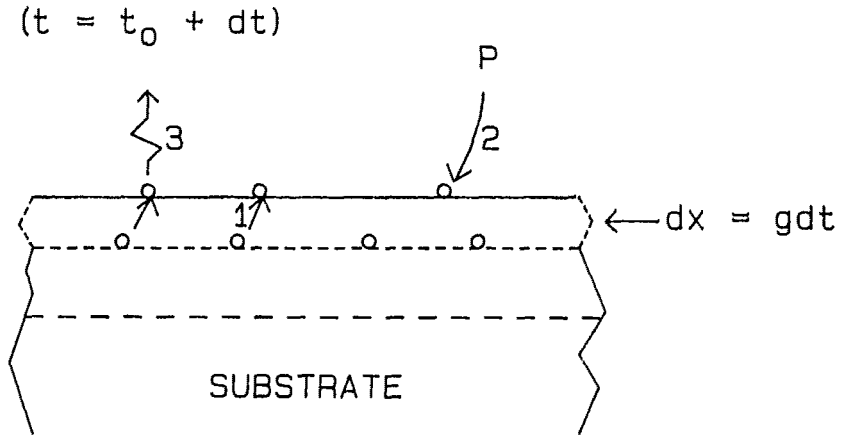


FIGURE 1: GROWING EPITAXY.



- 1: RELAXATION OF SURFACE ADSORBED ATOMS ( $F$ ).
- 2: ADSORPTION FROM GAS STREAM ( $k_{mf}$ ).
- 3: DESORPTION OF RELAXED ATOMS ( $k_v$ ).

FIGURE2: DEPOSITION OF SILICON.

The amount of impurities relaxed,  $N_A^r$ , onto the "new" surface is given by the density of impurities adsorbed on the "old" surface,  $N_A^o$ , less the amount trapped in the layer  $dx$ :

$$\begin{aligned} (3): N_A^r &= N_A^o - C_s dx \\ &= N_A^o - fN_A^o g dt \\ &= N_A^o [1 - gf dt] \end{aligned}$$

Let the change in adsorption density due to desorption and adsorption be denoted by  $dN_A^g$ , then the density of impurities,  $N_A^n$ , adsorbed on the "new" surface is given by:

$$\begin{aligned} (4): N_A^n &= dN_A^g + N_A^r \\ &= dN_A^g + N_A^o [1 - gf dt] \end{aligned}$$

Let  $dt$  tend to zero, and the following differential equation, basically a mass balance equation, can be derived:

$$(5): \frac{dN_A}{dt} = \frac{dN_A^g}{dt} - gfN_A$$

where  $N_A^o$  has been replaced by  $N_A$ .

It is assumed that  $dN_A^g/dt$  is related to the surface adsorption density ( $N_A$ ), and the partial pressure ( $P$ ) of dopant carriers in the gas stream through a first order kinetic equation:

$$(6): \frac{dN_A^g}{dt} = k_{mf}P - k_v N_A$$

where  $k_{mf}$  and  $k_v$  are the transport and desorption coefficients associated with the adsorption and desorption processes, respectively.

Combining equations (5) and (6):

$$(7): \frac{dN_A}{dt} + [k_v + gf]N_A = k_{mf}P$$

Since the thickness of the epitaxial layer ( $x$ ) is related to the growth rate ( $g$ ) by  $g = dx/dt$ , then by applying the chain rule, equation (7) can be transformed to:

$$(8): \frac{dN_A}{dx} + N_A \frac{k_v + gf}{g} = \frac{k_{mf}}{g} P$$

The transient response of the system is characterized by the length defined below:

$$(9): x_m = \frac{g}{k_v + gf}$$

$x_m$  represents the spatial extent of the transient in the epitaxial layer.

Using this definition of the transition width  $x_m$ , equation (8) can be rewritten in the following simplified form:

$$(10): \frac{dN_A}{dx} + \frac{N_A}{x_m} = \frac{k_{mf}}{g} P$$

For time independent dopant carrier partial pressure, and constant growth rate, the most general solution to equation (10) is given by:

$$(11): N_A = \left( N_A^0 - \frac{x_m k_{mf}}{g} P \right) \exp\left(-\frac{x}{x_m}\right) + \frac{x_m k_{mf}}{g} P$$

The first term on the right hand side of equation (11) represents the transient response, and the second term represents the steady state response. This neglects transients associated with establishing a steady state growth rate [5].

With the spatial variation of the surface adsorption density determined, that of the doping concentration,  $C_s$ , is then given by the product of  $N_A$  and  $f$  (equation (2)).

The steady state concentration in the epitaxial layer is particularly useful in the comparison of experimental data and the predictions of the model:

$$(12): C_{s.s.} = \frac{x_m k_{mf}}{g} fP$$

where  $C_{s.s.}$  is the steady state doping level in the epitaxial layer.

Substituting equation (9) into equation (12), and after appropriate rearrangements, the following equation is obtained:

$$(13): \frac{P}{C_{s.s.}} = \frac{1}{k_{mf}} \left[ g + \frac{k_v}{f} \right]$$

thus showing that if the trapping factor ( $f$ ) is independent of the growth rate ( $g$ ), then the ratio  $P/C_{s.s.}$  is linearly related to  $g$ . [4]

### 3: AUTODOPING

#### 3.1: modeling autodoping

We propose that the same mechanism that gives rise to transient effects in dopant incorporation processes is also responsible for autodoping. The equation for autodoping is simply equation (11) (with the dopant carrier partial pressure  $P$  set to zero):

$$(14): C_{\text{autodoping}} = f N_A^0 \exp\left(\frac{-x}{x_m}\right)$$

where  $N_A^0$  is the surface adsorption density immediately before deposition is carried out.

Though the ultimate origin of the impurities giving rise to autodoping is the highly doped substrate, this model regards the surface as the immediate source of impurities that dope the epitaxial layer.

It may be helpful to think of the surface as a "reservoir" partially "filled" with impurities even before deposition. During deposition, the reservoir gradually releases the stored impurities, and (auto)dopes the epitaxy.

Unlike autodoping on uniformly doped substrates, autodoping in substrates containing buried layers cannot be reduced to a one-dimensional problem. This is because the distribution of initial surface adsorption densities  $N_A^0$  now depends on the position relative to the buried layers. One might also suspect that during deposition, the "off" buried layer regions might be doped by impurities evaporated from the "on" buried layer regions. In other words, there could exist a position and time dependent dopant carrier partial pressure  $P$ . This higher dimensionality of autodoping in the presence of buried layers makes it inherently more difficult to be modelled.

To reduce the complexity of the problem, it is assumed that, compared to the contribution to autodoping through the trapping of impurities originally adsorbed on the surface before deposition, the corresponding contribution by impurities coming in from the gas phase during deposition is negligible (i.e.  $P = 0$ ). Therefore the modeling of autodoping in the more general case involving buried layers can be divided into two steps: lateral transport for the determination of  $N_A^0(x,y)$  before deposition, and autodoping profiling during deposition.

Two general consequences arise from the proposed mechanism of autodoping. First of all, the deposition parameters have only a partial influence on the autodoping profiles. Specifically, the transition width,  $x_m$ , but not the initial adsorption density,  $N_A^0$ , is affected by these parameters.  $N_A^0$  is determined by lateral transport during the pre-deposition baking process.

Secondly, the model assumes that most of the impurity atoms giving rise to lateral autodoping come from atoms adsorbed on the surface of the wafer before deposition. Consequently, the total integrated dose of autodoping cannot exceed the density of impurities originally adsorbed on the surface.

Moreover, the amount of impurities adsorbed is limited by the number of adsorption sites available on the surface. One can naively estimate the number of adsorption sites to be approximately  $10^{15} \text{ cm}^{-2}$  by assuming that there is one adsorption site associated with every surface atom. This implies that in the absence of significant re-deposition of evaporated impurity atoms (as is assumed in the model), no autodoping profiles can have integrated doses larger than  $10^{15} \text{ cm}^{-2}$ . Of all the autodoping profiles investigated in this work, the integrated doses (in excess of the background doping) all fall well below the proposed limit.

In summary, we have identified the phenomenon of autodoping as a transient effect of the dopant incorporation process. Profiles of autodoping "on" and "off" the buried layer can be generated by giving the initial surface adsorption densities.

### 3.2: pre-deposition baking and lateral transport

In most processing procedures, the wafers are subjected to a period of high temperature pre-deposition baking, sometimes accompanied by hydrogen chloride purging. It is expected that the surface adsorption density be affected by this process.



Our model assumes the relationship:

$$(15): C_o = fN_A^o$$

between the autodoping peak concentration  $C_o$  and the initial surface adsorption density  $N_A^o$ .

Intimate knowledge of the effects of the pre-deposition baking on the surface adsorption densities is required for quantitative predictions of autodoping profiles.

Figure 3 summarizes the possible destinations for the impurities coming out of the buried layer, and their relationship to "on" and "off" buried layer autodoping. Some impurities desorb and some do not. Those remaining on the top of the buried layer are responsible for "on" buried layer autodoping. Among the desorbed impurities, some are re-deposited on the surface away from the buried layer after being transported in the main gas stream. These impurities are responsible for "off" buried layer autodoping. The rest of the desorbed impurities simply leave the system and do not contribute to autodoping.

The exact distribution of the surface adsorbed impurities is a function of many variables. They include, for example, the velocity of and the flow pattern in the main gas stream, the diffusion coefficient of the impurity atoms in the carrier gas, the process conditions during pre-deposition baking, the geometry of the reactor, and the distribution of the buried layers, etc.

Gas phase transport analyses for a variety of heavy doping patterns have been carried out by Srinivasan. [6], [7]

#### 4: EXTRACTION OF PARAMETERS

In this section, the method for determining the deposition parameters  $k_{mf}$ ,  $k_v$ , and  $f$  is described.

Equation (13) indicates how useful information about the deposition parameters can be extracted by studying the steady state concentrations, entirely independent of the effects of autodoping.

The procedure involves first performing a series of steady state deposition experiments with different growth rates, other process parameters being kept constant. The quantity  $P/C_{s.s.}$  is calculated and plotted against growth rates. The model predicts (equation (13)) that the resulting plot should be a straight line with slope (m) and intercept (b) given respectively by:

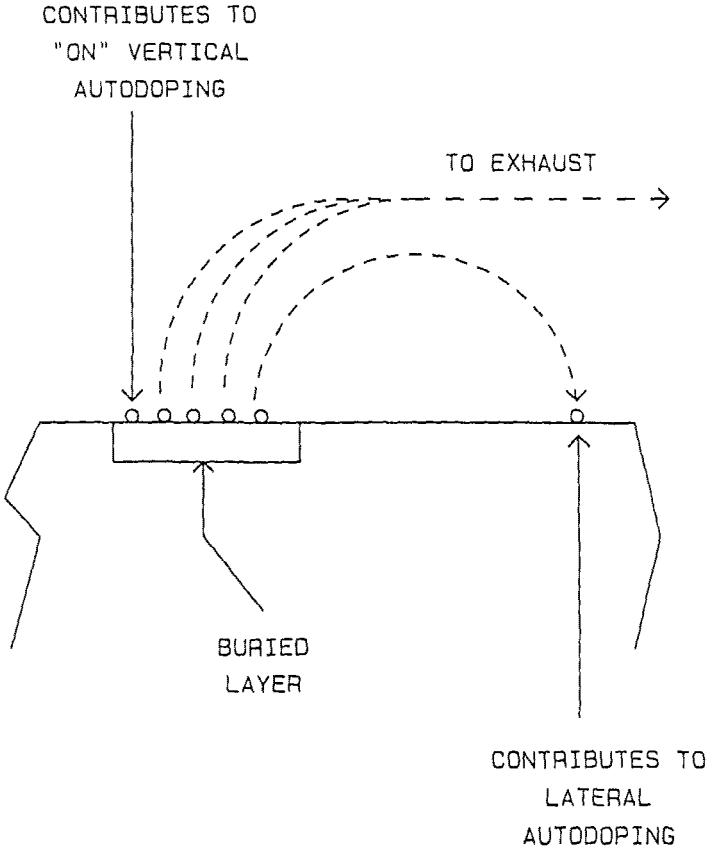


FIGURE 3; ORIGIN OF IMPURITIES.

$$(16): m = \frac{1}{k_{mf}}$$

$$(17): b = \frac{k_v}{k_{mf}} f$$

The transport coefficient  $k_{mf}$  is determined immediately from the slope:

$$(18): k_{mf} = \frac{1}{m}$$

On the other hand, the determination of the desorption coefficient  $k_v$  and the trapping factor  $f$  is not as straight forward. Equation (17) can be brought into the following form, more appropriate for the evaluation of these parameters:

$$(19): k_v = \frac{b}{m} f$$

Additional information needed for full specification of  $k_v$  and  $f$  can be obtained from transient doping profiles. These profiles (Figure 4) can be obtained by introducing a step change (Figure 5) in the dopant carrier partial pressure during deposition. The deposition is allowed to reach steady state both before and after the step is applied.

In principle, the initial slope, which is  $1/x_m$ , can be measured. This gives one more equation relating  $k_v$  and  $f$  (equation (9)), which together with equation (19), can be used to solve for the values of  $k_v$  and  $f$ . However, one can also use the following "simulation" method: equation (10) is solved to generate several simulated profiles, each with a different trapping factor (and the corresponding desorption coefficient  $k_v$  computed from equation (19)). This is illustrated in Figure 6.

The correct trapping factor must then generate both the best fitting profile and, via equation (19), the correct desorption coefficient  $k_v$ .

For lack of precise information on the surface adsorption densities, the following "method" of simulation is used. With the three deposition parameters already determined using the procedure outlined previously, several

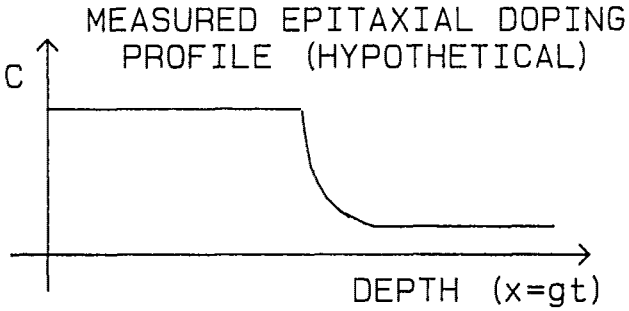


FIGURE 4: TRANSIENT PROFILE.

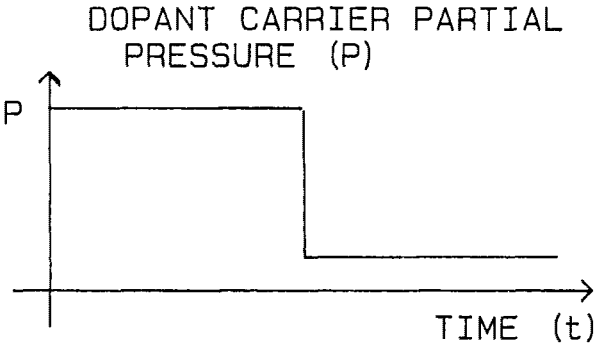


FIGURE 5: STEP CHANGE IN PRESSURE.

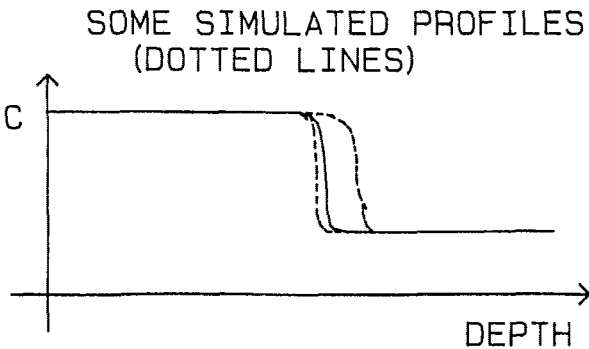


FIGURE 6: PARAMETER EXTRACTION.

autodoping profiles, each with a different initial surface adsorption density, are generated. The density that produces the best fit to the measured profile is taken to be the correct initial adsorption density. In fact, assuming the validity of the model, this number can be interpreted as a "measurement" of the local adsorption density just prior to deposition.

## 5: NUMERICAL IMPLEMENTATION AND COMPUTER SIMULATIONS

### 5.1: numerical implementation

Assuming the lateral transport mechanism is well modelled, the distribution of surface adsorbed impurities  $N_A^O(x,y)$  immediately before the deposition can be determined. Re-deposition from the gas stream during film deposition is completely neglected.

Regardless of the location of the point of interest with respect to the buried layers, autodoping profiles can be generated by using the local surface adsorption densities as initial conditions to the dopant incorporation equation. The phenomenon of solid state out-diffusion in the case of "on" buried layer autodoping has been well modelled by existing process simulators, e.g. SUPREM.

This procedure is summarized in Figure 7.

Figure 8 amplifies the box "Solve for Autodoping Profile" in Figure 7. Essentially, it shows how the numerical integration of the model equation (10) is carried out.

The choice of time step in the time increment box has to satisfy the inequality (A.6) in Appendix A.

### 5.2: computer simulations

Table 1 summarizes the deposition conditions for the simulated autodoping profiles shown in Figures 9 through 14.

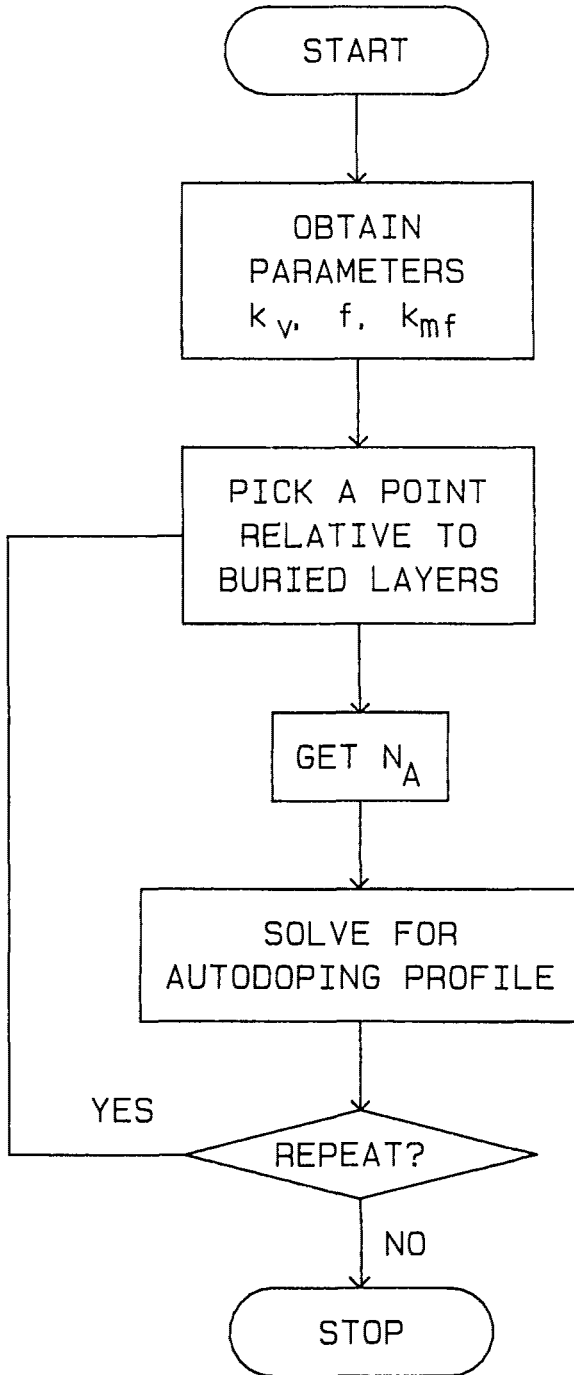


FIGURE 7: PROFILE GENERATION.

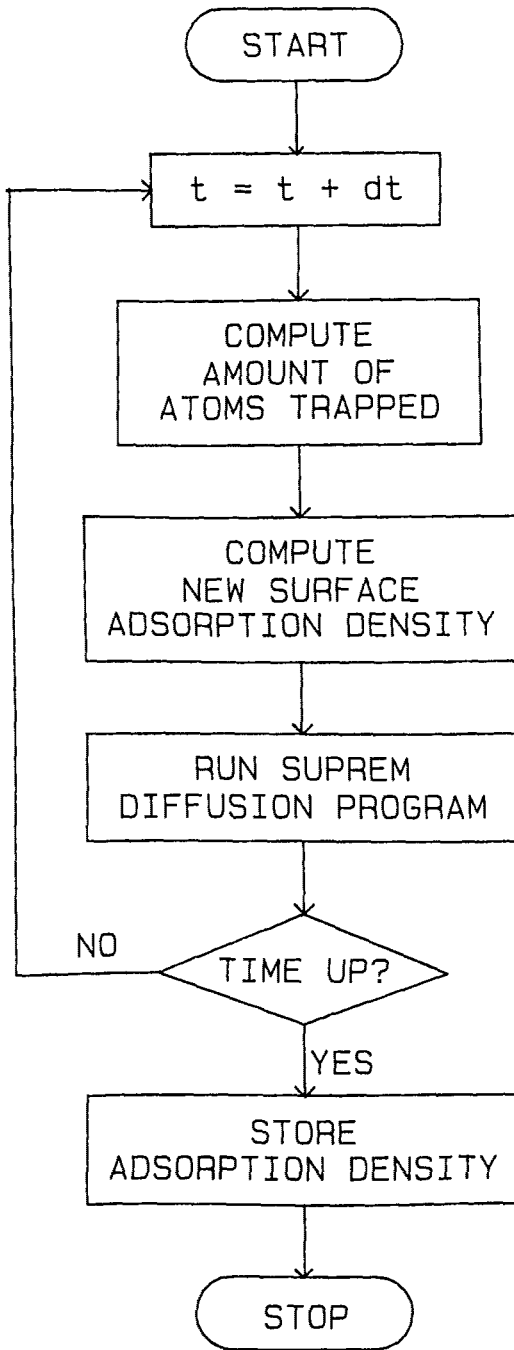


FIGURE 8: NUMERICAL INTEGRATION.

Table 1

<u>Figure</u>	<u>9</u>	<u>10, 11</u>	<u>12, 13, 14</u>
reactor	horizontal	barrel	horizontal
silicon carrier	SiH <sub>4</sub>	SiH <sub>2</sub> Cl <sub>2</sub>	SiCl <sub>4</sub>
deposition temp. (°C)	1050	1060	1150
deposition time (mins.)	15	12/15	20
growth rate (um/min)	.35	.3	.15
intended doping level (/cm <sup>3</sup> )	0.	2.0E15	0.
references	[4]	[1]/[2]	

Table 2 summarizes the deposition parameters used in the simulations.

Table 2

<u>Figure</u>	<u>9</u>	<u>10, 11</u>	<u>12, 13, 14</u>
k <sub>v</sub> (/s)	8.09E-3	1.32E-2	6.27E-3
f (/cm)	1.75E4	2.52E4	1.30E4

The initial surface adsorption densities N<sub>A</sub><sup>0</sup> used to generate the simulated profiles are summarized in Table 3:

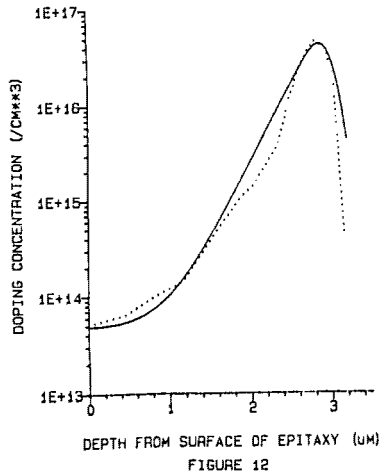
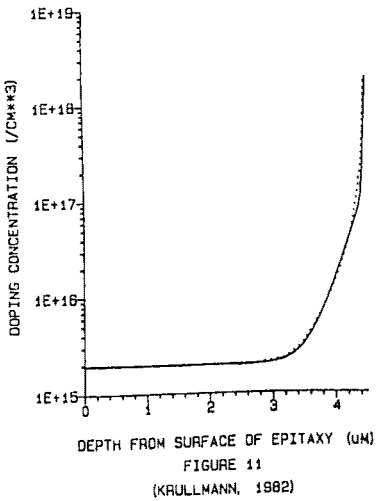
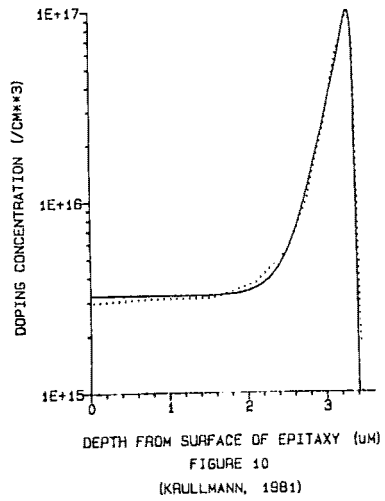
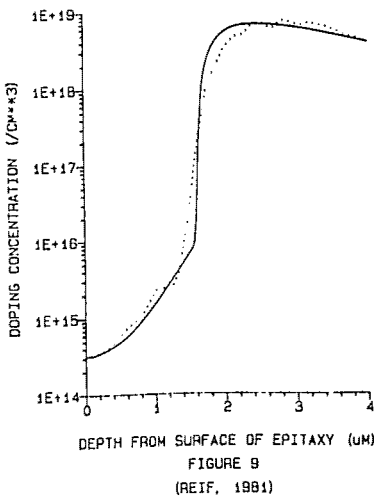
Table 3

<u>Figure</u>	<u>9</u>	<u>10</u>	<u>11</u>	<u>12</u>	<u>13</u>	<u>14</u>
adsorption density	6.0E11	5.4E12	5.8E12	6.4E12	4.9E12	4.0E12

Except for Figure 9, steady state information about the reactors for the other profiles is not available. This means that the values of the deposition parameters k<sub>mf</sub>, k<sub>v</sub>, and f are not known for these reactors. In order to curve-fit profiles in Figures 10 and 11, a relationship between k<sub>v</sub> and f is first obtained by measuring the slope of the "off" buried layer profile (Figure 10). Using the trapping factor for the profile in Figure 9 as a guide, one can then adjust the trapping factor and the initial



DOTTED LINE: MEASURED PROFILE  
 SOLID LINE: SIMULATED PROFILE



DOTTED LINE: MEASURED PROFILE  
SOLID LINE: SIMULATED PROFILE

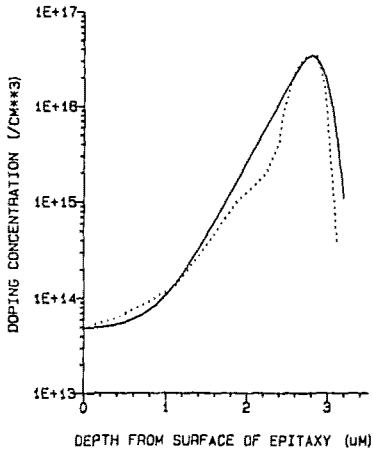


FIGURE 13

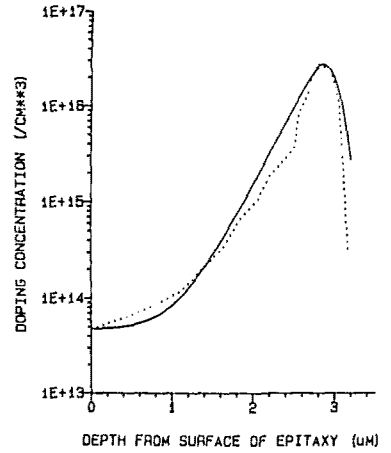


FIGURE 14

surface adsorption density to get the best fit to the "off" buried layer profile. The same  $k_v$  and  $f$  are then used to fit the "on" buried layer profile shown in Figure 11. This time, only the initial surface adsorption density is adjusted. The same procedure is carried out for simulating profiles in Figures 12, 13, and 14.

## 6: SUMMARY AND CONCLUSION

We presented a model of dopant incorporation in silicon epitaxy. The model equation is parameterized by three reactor dependent constants: transport coefficient  $k_{mf}$ , desorption coefficient  $k_v$ , and trapping factor  $f$ .

The pre-deposition baking process is parameterized by the initial surface adsorption density  $N_A^0$ . This parameter, when used as an initial condition to the model equation, enables vertical autodoping to be treated in a unified manner by the proposed model.

The model has been numerically implemented. It correctly predicts the experimentally observed exponential autodoping tail.

Autodoping profiles obtained from a variety of sources, representative of typical pre-deposition baking and deposition conditions, have been simulated. The fact that satisfactory profiles can be generated by properly specified parameters and initial surface adsorption densities strongly supports the proposed approach of modeling autodoping.

ACKNOWLEDGEMENT: This work is being supported by I.B.M. Corporation, U.S.A.

## REFERENCES

- [1] E. Krullmann, RWTH Aachen, PhD Thesis, p.81, 1981.
- [2] E. Krullmann, W. L. Engl, I.E.E.E. Transactions on Electron Devices, ED-29(4), p.491, 1982.
- [3] R. Reif, T. I. Kamins, K. C. Saraswat, Journal of the Electrochemical Society, 126(4), p.644, 1979.
- [4] R. Reif, R. W. Dutton, Journal of the Electrochemical Society, 128(4), p.909, 1981.
- [5] R. Reif, M. Vanzi, Journal of the Electrochemical Society, 128(10), p.2187, 1981.
- [6] G. R. Srinivasan, Journal of the Electrochemical Society, 127(10) p.2305, 1980.

[7] G. R. Srinivasan, Journal of Applied Physics, 51, p.4824, 1980b.

[8] M. Tabe, H. Nakamura, Journal of the Electrochemical Society, 126(5), p.822, 1979.

### APPENDIX A

If  $p$  denotes the probability that a given adsorbed atom is trapped when a monolayer of silicon is deposited, then after the deposition of  $n$  layers, the total amount of trapped impurities is given by:

$$(A.1): N_A^t = N_A [p + (1-p)p + \dots + (1-p)^{n-1}p]$$

where  $N_A^t$  is the amount of trapped impurities, and  $N_A$  is the amount of impurities adsorbed on the surface before any deposition.

This geometric series can be summed exactly:

$$(A.2): N_A^t = N_A [1 - (1-p)^n]$$

For  $p$  sufficiently small, the following approximation can be used:

$$(A.3): N_A^t = N_A np \\ = [N_A (p/u_0)] (nu_0)$$

where  $u_0$  is the thickness of a monolayer.

The following identifications can be made:

$$(A.4): f = p/u_0$$

$$(A.5): nu_0 = gdt = dx$$

In other words, the trapping factor can be interpreted as a probability per unit thickness, so that for thickness  $dx$ , the probability of an impurity atom being trapped is  $f dx$ .

Obviously, the approximation leading from (A.2) to (A.3) is valid only if the condition  $np \ll 1$  is satisfied. Therefore, for a given trapping factor, the increment  $dx$  must satisfy the following inequality:

$$(A.6): dx = nu_0 \ll 1/f$$